All-fibre photonic crystal distributed Bragg reflector (PC-DBR) fibre laser

J. Canning, N. Groothoff, E. Buckley, T. Ryan, K. Lyytikainen, J. Digweed

Optical Fibre Technology Centre & Australian Photonics Cooperative Research Centre, University of Sydney, 206 National Innovation Centre, ATP, Eveleigh, Sydney, NSW, 1430, Australia
Tel: 61-2-9351 1934, fax: 61-2-9351 1911,
j.canning@oftc.usyd.edu.au

Abstract: We describe an Er^{3+}-doped aluminosilicate core photonic crystal fibre laser incorporating distributed Bragg reflectors written by two-photon 193nm irradiation through an optical phase mask as the feedback elements. The laser is diode pumped at 980nm and evidence of dual linewidth laser operation close to threshold is observed. However, at higher pumping levels gain competition preferentially selects one laser line.

©2003 Optical Society of America

OCIS codes: (160.4670) Optical materials; (230.1150) All-optical devices (999.9999) Optical waveguides; (999.9999) Fresnel fibres; (999.9999) Scattering; (999.9999) Photonic crystal waveguides; (999.999) air-silica structured waveguides; (999.9999) fibre lasers; (999.999) lasers; (999.999) distributed Bragg reflector

References and links

1. D.P. Gapontsev, Presentation on High Power Fibre Lasers from IPG Photonics Corporation at LEAP Pavilion, Exhibit Hall, Conference on Lasers and Electro-Optics (CLEO 2003), Baltimore, USA, (2003)
2. K.P. Koo, A.D. Kersey, "Bragg grating-based laser sensor systems with interferometric interrogation and wavelength division multiplexing," J. Lightwave Tech. **13,** 1243-1249, (1995)
3. A. Asseh, H. Storoy, J.T. Kringlebotn, W. Margulis, B. Sahlgren, S. Sandgren, R. Stubbe, G. Edwall, "10 cm Yb3+ DFB fibre laser with permanent phase shifted grating," Electron. Lett. **31**, (12), 969-970, (1995)
4. D. Stepanov, J. Canning, L. Poladian, R. Wyatt, G. Maxwell, R. Smith, R. Kashyap, "Apodised distributed-feedback fibre laser," Opt. Fiber Tech. **5**, 209-214, (1999)
5. D. Yu. Stepanov, J. Canning, I. Basset, G.J. Cowle, "Distributed Feedback Ring All-Fibre Laser", *Trends in Optics and Photonics Series* (TOPS) **Vol. 1**, 291-295 (Optical Society of America, Washington D.C. USA), (1996)
6. E. Affolter, F.K. Kneubuhl, "Corrugated waveguide structure for distributed-feedback submillimeter-wave lasers," Phys. Lett. **58A,** 91-92, (1976)
7. H.P. Preiswerk, G. Kuttel, F.K. Kneubuhl, "Helical distributed feedback gas laser," Phys. Lett. **93A,** 15-17, (1982)
8. A. Michie, J. Canning, "Properties of a twisted DFB fibre laser", Post-deadline paper, Proceedings of Australian Conference on Optical Fibre Technology (ACOFT 2002), Darling Harbor Sydney, Australia, (2002); see patent: J. Canning, A. Michie, "Helical feedback laser operation in a linear DFB laser," PS2846
9. N. Groothoff, J. Canning, K. Lyytikainen, J. Zagari, "Gratings in air-silica structured fibre," Opt. Lett. **28**, 233-235, (2003)
10. W. J. Wadsworth, R. M. Percival, G. Bouwmans, J. C. Knight, and P. St. J. Russell, "High power air-clad photonic crystal fibre laser," Opt. Express **11**, 48- 53, (2003)
11. J. Limpert, T. Schreiber, S. Nolte, H. Zellmer, A. Tünnermann, R. Iliew, F. Lederer, J. Broeng, G. Vienne, A. Petersson, C. Jakobsen, "High-power air-clad large-mode-area photonic crystal fibre laser," Opt. Express **11**, 818-823, (2003)
12. J. Canning, M.G. Sceats, H.G. Inglis, P.Hill., "Transient and permanent gratings in phosphosilicate optical fibres produced by the flash condensation technique," Opt. Lett. **20**, 2189-2191, (1995)
13. J. Canning, P-F. Hu, "UV-induced losses in irradiated photo-hypersensitised optical fibres", In Press, Opt. & Las. In Eng., (2002)
14. J. Canning, "Contemporary Thoughts on Glass Photosensitivity and their Practical Application," Materials Forum **25**, 60-87, (2001)

#2641 - $15.00 US Received June 25, 2003; Revised August 14, 2003
(C) 2003 OSA

1. Introduction

Bragg gratings have played a substantial role in enabling practical utilisation of fibre lasers with diverse parameters, from narrow linewidths to kW powers [1]. Direct writing of gratings into active optical fibres has been particularly useful. For example, low power compact grating based lasers are increasingly underpinning ultra-high sensitivity sensor applications [2]. They can take many forms with a range of parameters determined by the application in mind. In particular, for sensor applications stable linewidths <10kHz and superior noise performance can be obtained using phase-shifted linear and ring distributed feedback (DFB) fibre lasers [3-5]. The flexibility in the surface area of fibre glass systems and their photosensitive response enables complex lasing phenomena to be generated that have not previously been observed in solid state lasers. One example is helical feedback operation (HFB) [6], previously only reported in gas lasers [7], but more recently generated in solid state form by twisting a DFB fibre laser after its fabrication or twisting prior to grating writing and subsequently releasing [8]. Thus gratings remain one of the key enabling technologies in photonic components. More recently, we have extended this capability to pure silica photonic crystal fibres that are not ordinarily photosensitive to standard grating writing methods [9]. Two-photon grating writing was shown to be feasible without requiring germanosilicate to be added to photonic crystal fibres, which would often compromise the distinguishing features of this fibre over conventional fibres. Further, in some lasing systems such as Yb:Er codoped optical fibres, germanosilica deleteriously impairs energy transfer efficiencies. In this paper we use this process to write grating pairs that form the resonator cavity in an air-silica structured fibre (commonly known as a photonic crystal fibre) laser doped with erbium and aluminium. Photonic crystal fibre lasers are a new area of research so far concentrating primarily on high power operation [10,11]. The possibility of combining the potential bandgap properties of photonic crystal fibres with those of longitudinal Bragg gratings promises to offer higher dimensional confinement solutions that can further tailor and refine the properties of passive and active filters, as well as fibre lasers for both low and high power operations.

2. Rare-earth doped photonic crystal fibre fabrication

The photonic crystal fibre is manufactured from a preform consisting of an array of capillaries drawn down to suitable dimensions. The light-guiding core region itself is fabricated by modified chemical vapour deposition (MCVD) within a silica preform collapsed such that the Er^{3+}-doped core is approximately 2mm in diameter. A total concentration of ~0.12wt% of Er_2O_3 is estimated from the measured absorption of 72dB/m at 1530nm. The additional incorporation of aluminium reduces clustering and promotes greater homogeneity of the rare

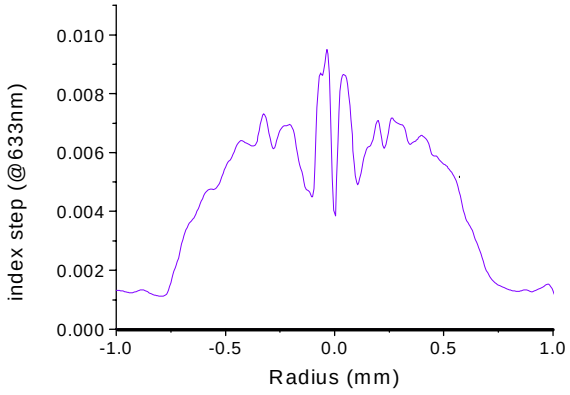

Fig. 1 Relative Index step from pure silica of preform core.

#2641 - $15.00 US
Received June 25, 2003; Revised August 14, 2003
(C) 2003 OSA

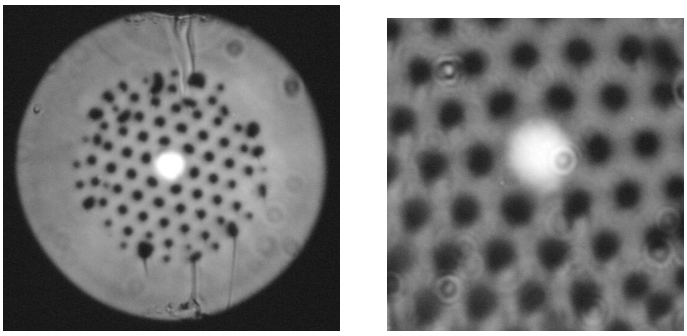

Fig. 2 White light transmission micrographs of cleaved 100μm diameter Er^{3+}aluminosilicate-core photonic crystal fibre. On the right hand side is a greater magnification of the core region.

earth. To remove excess silica, the outer silica layers are etched away using hydrofluoric acid until a solid Er^{3+}-doped aluminosilicate core surrounded by a thin layer of silica is obtained. The diameter of 2mm is chosen to be similar to the capillaries used. After etching, cleaning and drying, this core is inserted into the capillary stack. Figure 1 shows a cross-section of the preform core. The index step size arises from both the rare earth and the aluminium and is comparable to that used in conventional fibres, potentially posing some issues with respect to the propagation properties in the final fibre. This contribution can be removed or tailored by the addition of index-lowering dopants such as fluorine and boron.

Finally, the fibre itself is drawn down into three diameters: 125μm, 100μm and 70μm. Optical micrographs in transmission of the 100μm fibre are shown in Fig. 2. The doped core region is highlighted clearly where light seems to propagate as a result of the higher index. As expected an effective lower index silica ring arising from both the small layer of silica remaining after etching and the collapse of the first ring of interstitial holes between capillaries is observed. Comparison of the fluorescence spectra around 1550nm, obtained by pumping with 980nm, for the three fibres indicates that the confinement and coupling loss at 980nm is least in the 100μm fibre. Hence the reported results in this paper concentrate on the 100μm fibre. The core diameter is typically large – approximately 14μm diameter across the silica ring and approximately 8.4μm across the doped region in the 100μm fibre. Despite these dimensions the main propagation in these fibres at 1550nm is single "mode", since the leakage rate of the higher order modes is significant enough to ensure single "mode" propagation. This is based on calculations on a similar structure without an Er^{3+}-doped core where the fundamental loss is <20dB/km whilst the next highest mode loss is $>4x10^5$dB/km. This loss is compounded by the number of roundtrips within the resonator during lasing.

The small signal gain coefficient of the 100μm fibre was determined using standard cut-

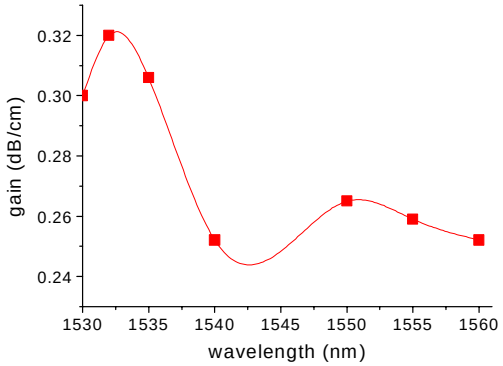

Fig. 3 Gain per unit length of Er^{3+}-doped aluminosilicate core photonic crystal fibre as a function of wavelength.

#2641 - $15.00 US Received June 25, 2003; Revised August 14, 2003
(C) 2003 OSA

back techniques. Pumping with 980nm through a wavelength division multiplexer (WDM) from one end whilst sending an appropriate tuneable laser signal wavelength from the other end through another WDM, allowed the gain profile per unit length as a function of wavelength to be extracted. The results are shown in Fig. 3.

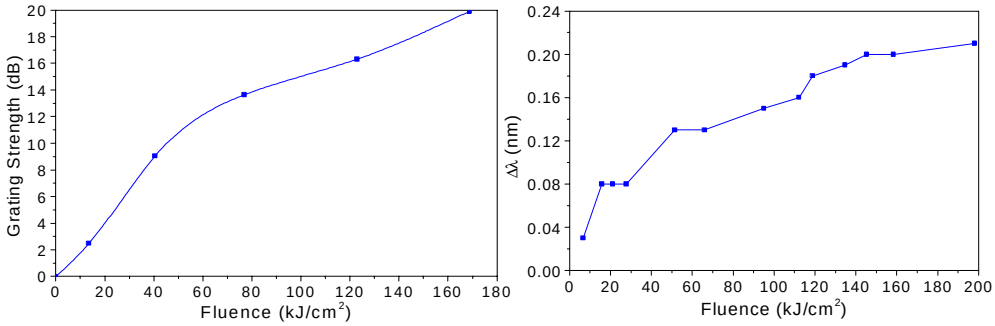

Fig. 4. Typical characteristic grating growth curves for grating in Er^{3+}-doped aluminosilicate core photonic crystal fibre. Grating strength as a function of fluence is shown on the left and

3. Grating writing

We follow previous work demonstrating strong grating writing in pure silica photonic crystal fibres using 2-photon irradiation through an optical phase mask. 193nm single-photon grating writing in non-germanosilicate glasses is also feasible when hydrogen loading is employed [12]. However, the use of hydrogen under normal writing conditions produces unwanted OH formation that reduces the Er^{3+} lifetime and hence the effective gain of the fibre. Whilst hypersensitisation methods can reduce losses [13,14], the presence of capillaries meant some effort is required to determine the optimum hypersensitisation fluence. Consequently, we decided to pursue the 2-photon grating writing method using an ArF exciplex laser and direct writing through an optical phase mask to produce 1cm gratings.

The characteristic grating growth curves for two-photon grating writing in the Er^{3+} doped aluminosilicate core photonic crystal fibre are shown in figure 4. From the wavelength shift a total UV-induced index change of ~$2x10^{-4}$ has been obtained using two-photon excitation of these fibres. No evidence of saturation is observed. Figure 5 shows a typical grating spectral profile of the type of grating used in the photonic crystal fibre lasers. This was measured using an erbium doped fibre amplifier as the broadband source through a short piece of fibre (2cm) to reduce the absorption. Whilst the fluences for multi-photon grating writing are generally higher than conventional single-photon grating writing, the use of both germanate and

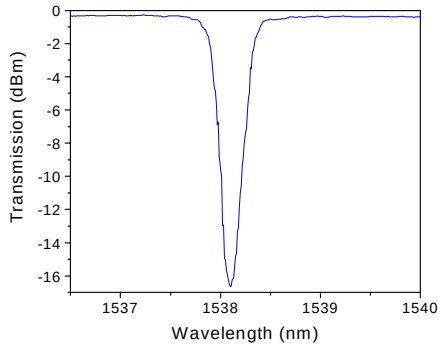

Fig. 5. Typical spectra of gratings in Er^{3+}doped aluminosilicate core photonic crystal fibre used as laser feedback elements.

#2641 - $15.00 US
Received June 25, 2003; Revised August 14, 2003
(C) 2003 OSA

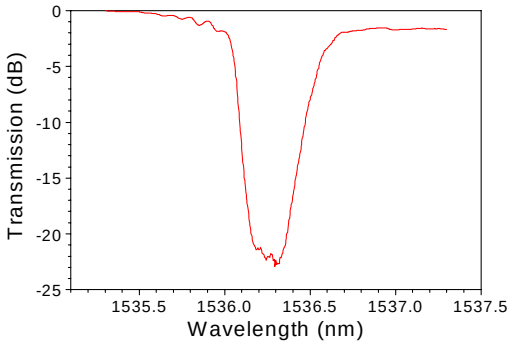

Fig. 6. Transmission spectra of distributed Bragg reflector (DBR) resonator.

hydrogen has been avoided. For our laser we chose two grating strengths: ~15dB for the input grating and ~9dB for the output grating. The cavity length inbetween is ~17cm. These values can be varied to both manipulate the threshold and slope efficiency of the laser. A spectrum of the two gratings in transmission through about 20 cm of fibre (noting that absorption is present) is shown in Fig. 6.

4. The photonic crystal distributed Bragg reflector (PC-DBR) fibre laser

The cavity length of our final laser is ~17cm inbetween gratings. Figure 7 shows a schematic of one type of configuration employed. The resonator was pumped through a wavelength division multiplexer (980/1550 WDM). The evolution of the laser signal at the output end as a function of pump current is shown in Fig. 8. Near threshold there is an onset of lasing at 1536.3nm close to the peak of the gain curve. However, a second laser mode at slightly longer wavelengths (1536.6nm) with a higher threshold appears and at a pump current of ~140mA dual laser line operation is observed. As the pump power is turned up, however, this second mode dominates and suppresses the first mode. This result is explained by the observation of a weaker grating in the silica surrounding the doped core region after grating writing. Since the index is lower, during grating writing the effective Bragg wavelength is less than that of the core region resulting in an apparent second grating within the silica ring. The index difference between core and silica ring (~0.008 – Fig. 1), with some contribution from the air-hole cladding, is consistent with the difference in wavelength between the two lasing modes. The mode field at 1530nm overlaps with this grating and hence some feedback is possible. Whilst the grating strengths, and therefore the cavity Q, is weaker than the core where the overlap is greater, the gain at this slightly shorter wavelength is higher (see Fig. 3) and accounts for the lower lasing threshold. At high pump powers above the thresholds for both modes, the greater overlap with the core grating ensures the higher cavity Q of the second mode eventually dominates the slightly higher gain of the first mode. Gain competition begins to favour the second mode leading to a depletion and suppression of the first mode.

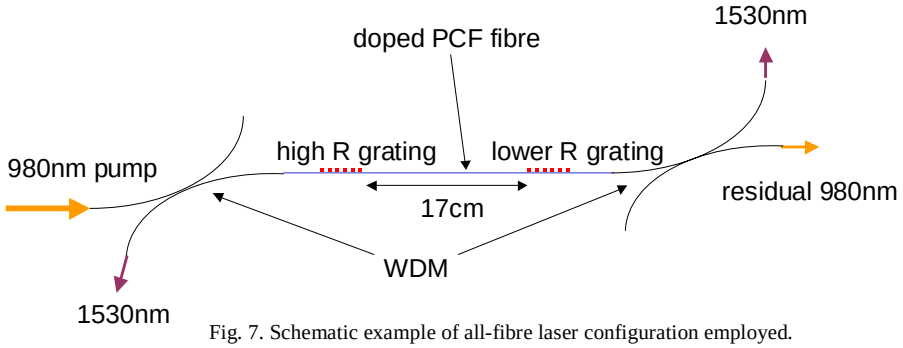

Fig. 7. Schematic example of all-fibre laser configuration employed.

#2641 - $15.00 US
Received June 25, 2003; Revised August 14, 2003
(C) 2003 OSA

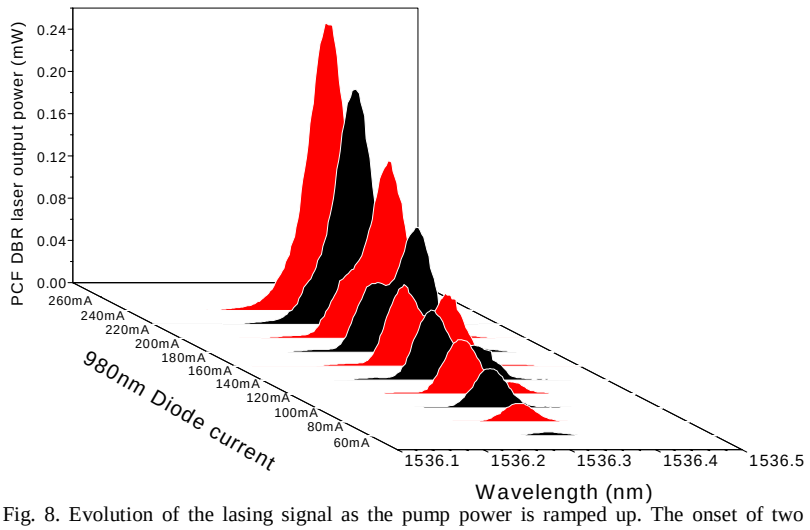

Fig. 8. Evolution of the lasing signal as the pump power is ramped up. The onset of two primary lasing modes is observed – one at a significantly lower threshold than the other.

The laser characteristic curve is shown in Fig. 9. The difference in thresholds and slope efficiencies for both modes are noticeable – the first mode has a pump threshold of about 28mW and a slope efficiency of ~0.3% whilst the second mode has a threshold of 44mW and slope efficiency of ~1%. The low slope efficiencies and some of the observed mode hopping at higher powers are partly attributable to pump multi-moded operation and pump confinement in both the undoped and doped regions of the core. Both these factors can be improved.

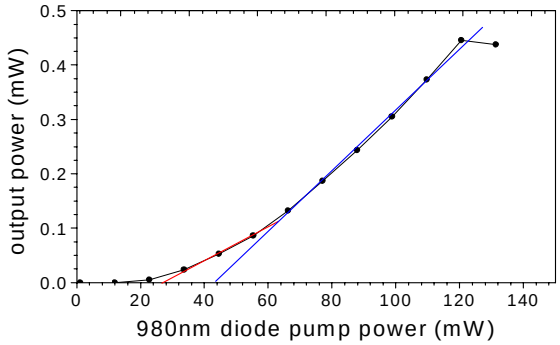

Fig. 9. Characteristic laser curve for the photonic crystal fibre DBR laser.

5. Conclusions

In conclusion, we have reported the first photonic crystal fibre laser using distributed Bragg reflectors written directly into the active fibre. Multi(two in this case)-photon grating writing enables gratings to be written without the need for complex dopant formulas or the use of hydrogen that may compromise the lasing performance of the device.

Acknowledgements

This work was funded by an Australian Research Council (ARC) Discovery Grant. Support of a J.G. Russell Award from the Australian Academy of Sciences is acknowledged.